

**Dynamics of hot-electron scattering in GaN heterostructures**

P. Tripathi and B. K. Ridley

*Department of Electronic Systems Engineering, University of Essex, Colchester, United Kingdom*

(Received 15 May 2002; published 1 November 2002)

A detailed comparison is made between the hot-electron rates for energy and momentum relaxation in electron-acoustic-phonon scattering and energy and momentum exchange rates in electron-electron scattering in a GaN heterostructure. In the case of piezoelectric scattering full account is taken of the anisotropy of the interaction and corresponding form factors have been calculated. The interaction with acoustic phonons is assumed to be statically screened. Dynamic screening of the electron-electron interaction is shown to give rise to resonances associated with plasmon-phonon coupled mode effects with overall dynamic rates rather insensitive to electron density at least for densities around  $1 \times 10^{12} \text{ cm}^{-2}$ . At these densities electron-electron scattering easily dominates the energy and momentum distribution at energies below the optical-phonon energy and is comparable with the optical phonon contribution above the phonon energy. The condition for the formation of a drifted Maxwellian distribution is discussed.

DOI: 10.1103/PhysRevB.66.195301

PACS number(s): 73.40.Cg, 63.20.Kr, 72.10.Di, 72.20.-i

**I. INTRODUCTION**

A comprehensive understanding of the electronic processes underlying the transport properties of GaN heterostructures is an essential requirement for the successful modeling of high-power microwave FET's and other devices. Although much of the basic physics can be carried over from previous work on GaAs, and even Si, heterostructures, not all of it can because GaN, though still tetrahedrally bonded, crystallizes in the wurtzite structure rather than the zinc blende structure of GaAs and, moreover, it is more strongly polar than GaAs. The lower symmetry of wurtzite allows the appearance of spontaneous electric polarization which results in the spontaneous creation of a neutralizing electron or hole gas at the heterostructure interface.<sup>1</sup> Although not as strong as in typical ferroelectrics, the spontaneous polarization is strong enough to induce carrier densities of  $10^{12}$ – $10^{13} \text{ cm}^{-2}$  without the necessity for doping.<sup>2,3</sup> In principle therefore, though rarely in practice, impurity scattering can be ignored, which makes the nitride system unique among semiconductor structures. This would suggest that at low temperatures, where phonon scattering is weak, mobilities of order  $10^6 \text{ cm}^2/\text{V s}$  may be expected, mirroring the record electron mobilities of around  $10^7 \text{ cm}^2/\text{V s}$  observed in the lighter effective mass GaAs structures. The low-temperature mobilities observed in state-of-the-art nitride high-electron-mobility transistors (HEMTS) is, however, an order of magnitude less. The discrepancy may not be due to the obvious culprit—interface roughness scattering—but rather to the fields produced by fluctuations in the dipole distribution in the barrier.<sup>4</sup> Nevertheless, dipole-scattering-limited mobilities are high enough for this type of scattering to be negligible at most temperatures of interest. Ordinary alloy scattering would have to be considered also where the barrier is small enough for there to be significant penetration of the electron wave function into the barrier, but even here the effect is predicted to be negligible in AlGaIn.<sup>5,6</sup> Improvements in crystal growing, reducing the effects of interface roughness and dislocations, encourages the study of electronic processes to focus purely on electron-phonon and

electron-electron interactions, and this is our aim here.

The interaction between electrons and optical phonons via the Fröhlich interaction, being the most important at temperatures above about 100 K in GaN, has properly been the subject of many papers in the literature. In wurtzite, unlike zinc blende, the interaction is anisotropic and involves both longitudinally and transversely polarized components.<sup>7</sup> The angular dependence of the coupling coefficients can be obtained simply for the case of weak anisotropy<sup>8</sup> and it turns out that the contribution from the TO modes is two orders of magnitude smaller than the contribution from the LO modes.<sup>9</sup> Most authors therefore adopt an isotropic, zinc blende-like, model. At an interface, the incident bulk GaN modes must satisfy mechanical and electrical boundary conditions. Because of the usually large disparity of atomic mass factors (such as the ratio of the reduced mass to the unit cell mass) at the interface the appropriate mechanical boundary condition is the vanishing of the optical displacement ( $\mathbf{u}=0$ ) (Ref. 10) corresponding to total reflection. The LO modes are therefore half-space modes. In addition there are interface modes. When the barrier is composed of a ternary alloy, such as in the AlInN/GaN system, there are three interface modes.<sup>11</sup> Satisfying the boundary conditions leads to the hybridization of all the modes<sup>12</sup> and complicates the calculation of scattering rates. Though essential for describing Raman scattering, hybridization can be sacrificed without much error in favor of the dielectric continuum (DC) model, which uses only electrical boundary conditions, when only electron scattering rates are required. An even simpler approximation, much adopted after its use in the AlAs/GaAs system,<sup>13</sup> is to forget about half-space and interface modes and simply use the bulk phonon spectrum; errors are rarely larger than 15–20%. The large electron densities typically obtained also require taking into account degeneracy, and the effect of Pauli exclusion was expected to reduce the rate. Solution of the linearised Boltzmann equation for the AlN/GaN system showed instead that the rate tended at first to increase as more electrons in the Fermi tail acquired enough energy to emit an optical phonon and only at higher Fermi energies did the rate decrease, with the result that the mobility reached a minimum at a density of  $10^{13} \text{ cm}^{-2}$ .<sup>14</sup>

With the possible exception of coupled-mode effects, scattering of electrons in GaN channels by polar optical phonons appear to be reasonably well understood. The large electron densities, even if short of degeneracy, will play an important role in screening, in providing plasmons and in determining the form of the distribution function at all electric fields. Needless to say, electron-electron scattering in GaAs channels has been the subject of too many papers to mention all here. One of the features of many is the common assumption of static screening of all interactions (e.g., Ref. 15), which is valid for all elastic interactions but not for inelastic scattering such as electron-electron interaction itself and for the interaction with optical phonons. Nevertheless, the need for dynamic screening of the electron-electron interaction is well pointed out.<sup>16,17</sup> In calculations of transport in GaN quantum wells, electron-electron scattering was, with one exception, not considered.<sup>18-21</sup> The exception was an analysis of moderately low temperature hot-electron transport where unscreened electron-electron scattering was taken to be strong enough to engender a drifted Maxwellian distribution, resulting in a number of novel phenomena including absolute cooling of electrons and squeezed electrons.<sup>22</sup> These results have contributed substantially to the motivation for this study. One of our aims, in short, is to examine the possibility of obtaining a hot-electron drifted Maxwellian distribution.

The regime of electron energies below the optical-phonon band is characterized in our ideal system by the dominance of scattering by acoustic modes, which accounts for both momentum and energy relaxation of hot electrons. In the strongly polar nitride systems, piezoelectric scattering, at low energies, is more intense than deformation-potential scattering, given the accepted values of the deformation constant. Piezoelectric scattering is highly anisotropic, particularly in wurtzite. Usually, some sort of spherical average is taken. However, form factors that incorporate the angular anisotropy have long been known for the zinc blende case<sup>23</sup> and they have been applied to GaAs (Ref. 15) and even to GaN.<sup>19</sup> As far as the authors are aware, form factors incorporating the wurtzite anisotropy, derived in this paper, have not been given before.

As regards the electron-electron interaction, the details of energy-exchange in the presence of dynamic screening have not been explored; where dynamic screening has been considered (e.g., Ref. 16) the emphasis has been on scattering rates. Our interest here is less on the scattering rates themselves, more on the dynamical aspects, i.e., momentum exchange and energy exchange, since it is these that must be compared with the rates of momentum relaxation and energy relaxation associated with the interaction with phonons and which determine the form of the distribution function for hot electrons.

## II. ACOUSTIC PHONON ENERGY

Below about 100 K in GaN the dominant process for relaxing hot-electron energy is via the interaction with acoustic phonons. In the 2D case these can be regarded validly as being essentially bulk travelling modes, complications asso-

ciated with the presence of an interface being discounted. The interaction with electrons is usually regarded as quasi-elastic, the phonon energies involved being much less than the electron energy. While this property is undoubtedly valid in bulk material, it is not necessarily so for quasi-2D electron gases. The phonon energy for long-wavelength modes is proportional to the wave vector  $\mathbf{Q}$ , i.e.,  $\hbar\omega = \hbar\mathbf{s}\cdot\mathbf{Q}$ , where  $\mathbf{s}$  is the velocity of sound, or simply  $\hbar\omega = \hbar sQ$ , taking spherical averages over the elastic anisotropy. In bulk material  $Q$  is determined by the conservation of crystal momentum, which limits the magnitude to roughly  $0 \leq Q \leq 2k$ , where  $k$  is the electron wave vector, and since  $k$  corresponds to long wavelengths in most cases in semiconductor physics, so does  $Q$  and the energy is correspondingly small. In the 2D case momentum conservation is limited to the in-plane component  $q$  and no such restriction applies to the perpendicular component  $q_z$ . The phonon energy is therefore not so precisely determined since  $\hbar\omega = \hbar s(q^2 + q_z^2)^{1/2}$ . The only limitation on  $q_z$  is provided by the modulus squared overlap integral  $|G(q_z)|^2$ :

$$G(q_z) = \int \psi(z)^2 e^{iq_z z} dz, \quad (1)$$

where  $\psi(z)$  is the  $z$  component of the electron wave function. An approximate form for the latter for the ground state in a heterostructure channel is the Fang-Howard wave function:<sup>24</sup>  $\psi(z) = (b^3/2)^{1/2} e^{-bz/2}$ , in which case  $|G(q_z)|^2$  falls off rapidly for  $q_z \geq b/2$

$$|G(q_z)|^2 = \frac{b^6}{(b^2 + q_z^2)^3}. \quad (2)$$

For the deep square well case, the overlap integral falls off rapidly for  $q_z > 0$  and again, after a weak resonance, for  $q_z > 2\pi/a$ , where  $a$  is the well width. Thus, as long as the width of the well contains many monolayers, the error in ignoring the contribution to the phonon energy made by  $q_z$  will be small, thanks to the relatively small magnitude of the sound velocity, and the interaction can safely be taken to be quasielastic, as far as evaluating the scattering rate or the momentum relaxation rate is concerned. Another bonus of this approximation is that the screening of the interaction can be assumed to be static. In general, however, the usual assumption of the 2D rate being simply derivable from the 3D rate by multiplying by  $I(b)$ ,<sup>25</sup> where

$$I(b) = \int_{-\infty}^{\infty} |G(q_z)|^2 dq_z / 2\pi = 3b/16 \quad (3)$$

and  $3/2a$  in the case of a deep square well, is not strictly valid.

The problem becomes most acute in the evaluation of the energy relaxation rate, since the magnitude of the phonon energy emitted or absorbed is central to the calculation. However, for wells that are not too narrow it will be reasonable to obtain the energy relaxation rate with the approximation  $Q = q$ . For simplicity we will adopt this approximation and derive all rates with the usual assumptions of quasielasticity, energy directly proportional to  $q$  and lattice tempera-

tures high enough for equipartition to hold. Errors introduced will be unimportant as far as a comparison with energy exchange rates associated with electron-electron scattering since, as we will see, the latter are much bigger for the electron densities of interest. The procedure will, however, somewhat underestimate the true rates, which would lead to a slight underestimate of the electric field for the onset of warm-electron effects. However, our concern is the behavior

of hot electrons, where the relatively high energy of the electrons favors the approximation  $Q = q$ .

### III. DEFORMATION-POTENTIAL RATES

The scattering rate derived from Fermi's golden rule is

$$W(k) = \frac{\pi \Xi^2}{\rho \Omega} \int_{-\infty}^{\infty} dq_z |G(q_z)|^2 \frac{L_z}{2\pi} \int \frac{Q^2}{\omega(1+q_s/q)^2} \times \left\{ n(\omega) + \frac{1}{2} \pm \frac{1}{2} \right\} \delta_{\mathbf{k}', \mathbf{k} \pm \mathbf{q}} \delta\{E(k') - E(k) \mp \hbar \omega\} q dq d\theta \frac{L_x L_y}{4\pi^2}, \quad (4)$$

where  $\Xi$  is the deformation constant,  $\rho$  is the mass density,  $\Omega = L_x L_y L_z$  is the cavity volume,  $\omega = sQ$ ,  $n(\omega)$  is the Bose-Einstein factor, equal in this case to  $k_B T / \hbar \omega \gg 1$ , and  $q_s = e^2 n F(q) / (2\epsilon_s k_B T)$  is the 2D static screening factor with  $n$  = electron density,  $\epsilon_s$  is the static permittivity, and  $F(q) = (8 + 9r + 3r^2) / 8(1+r)^3$  with  $r = q/b$  is the form factor for the Fang-Howard wave function with only the ground state being occupied. We assume that the electrons are in a spherically symmetric conduction band and that they interact via the deformation potential only with longitudinally polarized acoustic (LA) modes. We also assume that the conduction band is parabolic.

We now apply the simplifying approximation  $Q = q$ , which allows us to carry out the integration over  $q_z$  [see Eq. (3)]. Performing the integration over angle gives

$$W(k) = \frac{3\Xi^2 m^* b}{32\pi \hbar^3 s^2 \rho k} \left[ \int_0^{2k(1+\eta)} \frac{k_B T}{(1+q_s/q)^2 \sqrt{1 - \{(q/2k) - \eta\}^2}} dq + \int_0^{2k(1-\eta)} \frac{k_B T + \hbar s q}{(1+q_s/q)^2 \sqrt{1 - \{(q/2k) + \eta\}^2}} dq \right], \quad (5)$$

where  $\eta = m^* s / \hbar k$ , and  $s$  is the velocity of longitudinally polarized acoustic (LA) modes. The first integral is for absorption, the second for emission. Retention of the small quantity  $\eta$  is essential for the calculation of energy relaxation.

The momentum relaxation rate is obtained by weighting the integrands with the factor  $q^2/2k^2$  and neglecting  $\eta$ :

$$W(k) = \frac{3\Xi^2 m^* b k_B T}{32\pi \hbar^3 s^2 \rho k^3} \left[ \int_0^{2k} \frac{q^2}{(1+q_s/q)^2 \sqrt{1 - (q/2k)^2}} dq \right]. \quad (6)$$

The energy relaxation rate is given by Eq. (5) with the integrands multiplied by the phonon energy and a change of sign of the second integral

$$W(E) = - \frac{3\Xi^2 m^* b}{32\pi \hbar^3 s^2 \rho k} \left[ \int_0^{2k(1+\eta)} \frac{\hbar s q k_B T}{(1+q_s/q)^2 \sqrt{1 - \{(q/2k) - \eta\}^2}} dq - \int_0^{2k(1-\eta)} \frac{\hbar s q (k_B T + \hbar s q)}{(1+q_s/q)^2 \sqrt{1 - \{(q/2k) + \eta\}^2}} dq \right]. \quad (7)$$

We evaluate the integrals numerically. The integrals can be evaluated analytically only if the  $q$  dependence of the form factor that determines the screening is ignored by adopting some average.

### IV. PIEZOELECTRIC RATES

In the piezoelectric interaction the coupling parameter for deformation-potential scattering  $\Xi^2 q^2$  is replaced by

$e^2 K_\alpha^2(\theta) c_\alpha(\theta) / \epsilon(\theta)$ , where  $K_\alpha(\theta)$  is the directionally dependent electromechanical coupling coefficient,  $c_\alpha(\theta)$  is the corresponding elastic constant, and  $\epsilon(\theta)$  is the permittivity. The subscript becomes  $L$  for longitudinally polarized modes and  $T$  for transversely polarized modes. The anisotropy of the piezoelectric, elastic, and dielectric properties make the calculation of scattering rates more complicated. It is usual to take spherical averages of the dielectric constants, i.e.,  $\epsilon = (\epsilon_{11} + \epsilon_{33})/2$ , and of the elastic constants<sup>25</sup>

$$c_L = \frac{1}{3}(2c_{11} + c_{33}) - \frac{2}{15}c_x,$$

$$c_T = c_{44} + \frac{2}{15}c_x,$$

$$c_x = c_{11} + c_{33} - 2c_{13} - 4c_{44}. \quad (8)$$

There are five nonzero piezoelectric coefficients  $e_{31} = e_{32}, e_{33}, e_{24} = e_{15}$ . For an acoustic wave traveling with polar coordinates  $r, \theta, \phi$  with the  $c$  axis as the polar axis there are three orientations of unit-cell displacement: (1) along the direction of travel (longitudinally polarized), (2) at right angles to the direction of travel in the plane containing the  $c$  axis (transversely polarized), and (3) at right angles to both the direction of travel and the plane containing the  $c$  axis (again transversely polarized). In the last case the displacement is in the basal plane of the hexagon and the piezoelectric interaction vanishes. For the other cases the effective coefficients are

$$e_L = e_{33} \cos^3 \theta + (e_{31} + 2e_{15}) \cos \theta \sin^2 \theta,$$

$$e_T = -(e_{33} - e_{31} - e_{15}) \cos^2 \theta \sin \theta - e_{15} \sin^3 \theta. \quad (9)$$

The dimensionless electromechanical coupling coefficients are

$$K_L^2 = \frac{e_L^2}{\varepsilon_x c_L}, \quad K_T^2 = \frac{e_T^2}{\varepsilon_s c_T}. \quad (10)$$

The scattering rate, with energy principally determined by the in-plane wave vector, is given by

$$W_\alpha(k) = \frac{e^2 m^*}{4\pi^2 \varepsilon_s \hbar^2 k} \times \int_0^{2k(1 \pm \eta)} \frac{F_\alpha(K_\alpha, T, q)}{(1 + q_s/q)^2 \sqrt{\{1 - [(q/2k) \mp \eta]^2\}}} dq, \quad (11)$$

where

$$F_\alpha(K_\alpha, T, q) = \int_{-\infty}^{\infty} dq_z \int_0^{\infty} dz \int_0^{\infty} dz' \psi^2(z) \psi^2(z') \times e^{iq_z(z-z')} C_\alpha^2(K_\alpha, T, q, q_z) \quad (12)$$

and

$$C_\alpha^2(K_\alpha, T, q, q_z) = K_\alpha^2 \left[ \frac{k_B T}{\hbar(q^2 + q_z^2)} + \left( \frac{1}{2} \mp \frac{1}{2} \right) \frac{s_\alpha}{\sqrt{(q^2 + q_z^2)}} \right] \approx \frac{K_\alpha^2 k_B T}{\hbar(q^2 + q_z^2)} \left[ 1 + \left( \frac{1}{2} \mp \frac{1}{2} \right) \frac{\hbar s_\alpha q}{k_B T} \right]. \quad (13)$$

In order to decouple the integration over  $q$  from that over  $q_z$  we have again assumed that the phonon energy is essentially determined by  $q$ . To express the polar angles in Eq. (9) in terms of the components of the phonon wave vector we assume that the plane of the channel is perpendicular to the  $c$  axis, which is the usual case in practice. In which case  $\cos \theta = q_z / \sqrt{q^2 + q_z^2}$  and the electromechanical coupling coefficient can be expressed as a function of  $q$  and  $q_z$ . The approximation in Eq. (13) allows the same form-factored coupling to apply to both stimulated and spontaneous processes.

In the calculation of the momentum relaxation rate the second term in the brackets of Eq. (13) is much smaller than the first and can be neglected. The integrations over  $q_z$  and  $z$  can then be carried out analytically, leading to the expressions below. The second term in Eq. (13) must be retained in the calculation of the energy relaxation rate. The phonon energy multiplying the first term is, however, approximated as usual ( $\hbar \omega \approx \hbar s_\alpha q$ ). The integrations over  $q_z$  and  $z$  can again be carried out analytically to give

$$F_\alpha(K_\alpha, T, q) = G_\alpha(K_\alpha, T, q) \left[ 1 + \left( \frac{1}{2} \mp \frac{1}{2} \right) \frac{\hbar s_\alpha q}{k_B T} \right],$$

$$G_L(K_L, T, q) = \frac{\pi k_B T}{\hbar \varepsilon_s c_L q} \left[ \begin{aligned} & e_a^2 \frac{1}{48} (15f_0 - 33f_1 + 12f_2 - f_3) + e_a e_b \frac{1}{4} (3f_0 - 5f_1 + f_2) \\ & + e_b^2 \frac{1}{2} (f_0 - f_1) \end{aligned} \right],$$

$$G_T(K_T, T, q) = \frac{\pi k_B T}{\hbar \varepsilon_s c_T q} \left[ e_a^2 \frac{1}{48} (3f_0 + 3f_1 - 6f_2 + f_3) + e_a e_{15} \frac{1}{4} (f_0 + f_1 - f_2) + e_{15}^2 f_0 \right]. \quad (14)$$

Here the  $f_n$  are form factors associated with the Fang-Howard wave function. They are defined in the Appendix. The piezoelectric coefficients appearing in Eq. (14) are  $e_a = e_{33} - e_b, e_b = e_{31} + 2e_{15}$ .

The momentum relaxation rate is

$$W_m(k) = \frac{e^2 m^* k_B T}{4 \pi \epsilon_s \hbar^3 k^3} \int_0^{2k} \frac{q [K_L^2(q) + K_T^2(q)]}{(1 + q_s/q)^2 \sqrt{1 - (q/2k)^2}} dq \quad (15)$$

and the  $q$ -dependent electromechanical coupling coefficients are given by

$$K_L^2(q) = \frac{1}{\epsilon_s c_L} \left[ \begin{array}{l} e_a^2 \frac{1}{48} (15f_0 - 33f_1 + 12f_2 - f_3) \\ + e_a e_b \frac{1}{4} (3f_0 - 5f_1 + f_2) + e_b^2 \frac{1}{2} (f_0 - f_1) \end{array} \right],$$

$$K_T^2(q) = \frac{1}{\epsilon_s c_T} \left[ e_a^2 \frac{1}{48} (3f_0 + 3f_1 - 6f_2 + f_3) + e_a e_b \frac{1}{15} (f_0 + f_1 - f_2) + e_b^2 \frac{1}{15} f_0 \right]. \quad (16)$$

In the case of energy relaxation the contributions from the LA and TA modes must be evaluated separately. The energy relaxation rate is given by

$$W(E) = - \frac{e^2 m^* k_B T s_\alpha}{4 \pi \epsilon_s \hbar^2 k} \left[ \begin{array}{l} \int_0^{2k(1+\eta_\alpha)} \frac{K_\alpha^2(q)}{(1 + q_s/q)^2 \sqrt{1 - \{(q/2k) - \eta_\alpha\}^2}} dq \\ - \int_0^{2k(1-\eta_\alpha)} \frac{K_\alpha^2(q) \{1 + (\hbar s_\alpha q / k_B T)\}}{(1 + q_s/q)^2 \sqrt{1 - \{(q/2k) + \eta_\alpha\}^2}} dq \end{array} \right]. \quad (17)$$

Once again the integrals have to be evaluated numerically.

Clearly, taking the piezoelectric anisotropy into account complicates the expressions considerably. It is interesting to compare the results of taking the anisotropy fully into account and the results using spherical averages<sup>26</sup>

$$\langle e_L^2 \rangle = \frac{1}{7} e_{33}^2 + \frac{4}{35} e_{33} (e_{31} + 2e_{15}) + \frac{8}{105} (e_{31} + 2e_{15})^2,$$

$$\langle e_T^2 \rangle = \frac{2}{35} (e_{33} - e_{31} - e_{15})^2$$

$$+ \frac{16}{105} e_{15} (e_{33} - e_{31} - e_{15}) + \frac{16}{35} e_{15}^2. \quad (18)$$

In the expression for the momentum relaxation rate the terms in the square brackets of Eq. (16) are replaced by  $\langle e_L^2 \rangle f_0$  and  $\langle e_T^2 \rangle f_0$ . The comparison of the effective  $q$  dependence in the case of GaN is shown in Fig. 1. The differences are significant.

## V. ELECTRON-ELECTRON RATES

For simplicity we will regard the rate of electron-electron scattering by electrons with the same spin as negligible because of exchange and interference effects. The energy exchange rate can then be obtained by ignoring spin and treating the interaction as a simple two-body collision in which an incident electron, wave vector  $\mathbf{k}_1$ , collides with a target electron, wave vector  $\mathbf{k}_2$ , and after collision the electrons have wave vectors  $\mathbf{k}'_1$  and  $\mathbf{k}'_2$ . We assume that the electrons remain in the lowest subband. The frequency of this process is calculated as usual in the Born approximation. The physi-

cally meaningful rates are momentum and energy exchange rates rather than simple scattering rates, which means that the order of summation must be such that the final sum should be over one of the final states suitably weighted by the amount of energy or momentum exchanged. The following calculation is of the rate of energy exchange. When the energy exchanged is significantly large the rate will be also equal to the momentum exchange rate.

The scattering rate for the process  $\mathbf{k}_1 \rightarrow \mathbf{k}'_1$  in an isotropic, Maxwellian distribution is

$$W(\mathbf{k}_1, \mathbf{k}'_1) = \frac{e^4 n}{8 \pi \hbar A N_d} \int e^{-E_2/k_B T} \frac{F^2(q)}{\epsilon(\mathbf{q}, \omega)^2 q^2} \times \delta(E'_1 + E'_2 - E_1 - E_2) 2 d\mathbf{k}_2, \quad (19)$$

where  $n$  is the areal density of electrons,  $N_d$  is the effective density of states in the lowest subband,  $A$  is the area,  $F(q)$  is

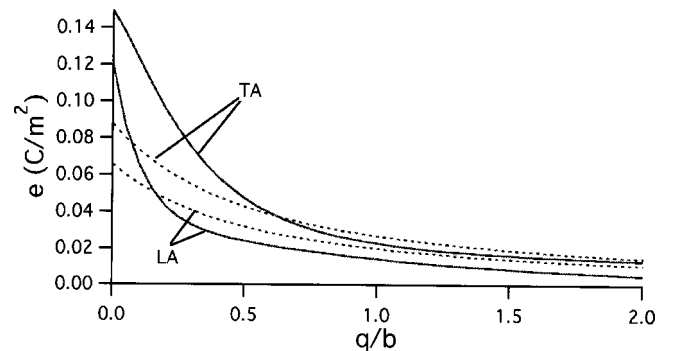


FIG. 1. Effective piezoelectric coefficients in GaN (full lines) compared with spherical-average approximation (dashed lines).  $q$  is the acoustic wave vector and  $b$  is the Fang-Howard factor.

the form factor [=  $f_0$ , Eq. (A1)],  $\hbar\mathbf{q}$  is the momentum transfer, and  $\varepsilon(\mathbf{q}, \omega)$  is the permittivity. Integration over  $\mathbf{k}_2$  is straightforward. The integral over the angle between  $\mathbf{k}_1$  and  $\mathbf{k}'_1$  can be expressed in terms of a new variable

$$u = \frac{q}{(k_1^2 - k_1'^2)^{1/2}} \quad (20)$$

so, after some manipulation and including the case for  $k_1 < k'_1$ , we get

$$W(k_1, k'_1) = W_0 \int_{\gamma}^{\gamma^{-1}} \frac{F^2(u)}{|\varpi|^{3/2} \{\varepsilon(u, \varpi)/\varepsilon_{\infty}\}^2} \times e^{\varpi/2} \frac{\exp\left\{-\frac{|\varpi|}{4}\left(u^2 + \frac{1}{u^2}\right)\right\}}{u^2 \left\{(u^2 - \gamma^2)\left(\frac{1}{\gamma^2} - u^2\right)\right\}^{1/2}} du, \quad (21)$$

$$W_0 = \frac{e^4 n \hbar}{8 \pi^{1/2} \varepsilon_{\infty}^2 m^* (k_B T_e)^2 A}, \quad \gamma = \left| \frac{k_1 - k'_1}{k_1 + k'_1} \right|^{1/2},$$

where  $\varepsilon_{\infty}$  is the high-frequency permittivity of the lattice and  $\varpi = (E_1 - E'_1)/k_B T_e$  is the normalized exchange energy. Equation (3) is just that derived by Esipov and Levinson,<sup>27</sup> but with the form factor and screening factor included. The energy-relaxation rate for the incident electron is then of the form

$$Q = \int (E_1 - E'_1) W(k_1, k'_1) k'_1 dk'_1 A / 2\pi. \quad (22)$$

Dynamic effects enter into screening via the factor  $\mathbf{q} \cdot \mathbf{v}_{\text{cm}}$ , where  $\mathbf{v}_{\text{cm}}$  is the velocity of the center of mass.<sup>28</sup> It is straightforward to show that this factor is nothing but  $(E_1 - E'_1)/\hbar$  which is the frequency associated with the energy loss by the incident electron.<sup>29</sup>

The permittivity is composed of the sum of lattice and electronic contributions. In a polar semiconductor the lattice contribution in the long-wavelength limit is

$$\varepsilon_L(0, \omega) = \varepsilon_{\infty} \frac{\omega^2 - \omega_{LO}^2 + i\omega\Gamma}{\omega^2 - \omega_{TO}^2 + i\omega\Gamma}, \quad (23)$$

where  $\Gamma$  is the decay rate. The electronic contribution can be obtained in the random-phase approximation neglecting the effects of exchange and correlation. A closed expression for the non-degenerate state has recently been obtained by Lee and Galbraith.<sup>16</sup> The real part is

$$\varepsilon_{eR} = \frac{e^2 m^* n F(q)}{2 \pi \hbar^2 N_d q^2} \left[ A_+ \Phi\left(1, \frac{3}{2}, -\frac{\hbar^2 A_+^2}{2 m^* k_B T_e}\right) + A_- \Phi\left(1, \frac{3}{2}, -\frac{\hbar^2 A_-^2}{2 m^* k_B T_e}\right) \right], \quad (24)$$

$$A_{\pm} = \frac{1}{2q} \left( q^2 \pm \frac{2m^*}{\hbar^2} \hbar\omega \right),$$

where  $N_d = m^* k_B T_e / \pi \hbar^2$  is the 2D density of states and  $\Phi(1, 3/2, -z)$  is a confluent hypergeometric function, and the imaginary part is

$$\varepsilon_{eI} = \frac{e^2 m^* n F(q)}{2 \pi \hbar^2 N_d q^2} \sqrt{\frac{\pi m^* k_B T_e}{2 \hbar^2}} \times (e^{-\hbar^2 A_-^2 / 2 m^* k_B T_e} - e^{-\hbar^2 A_+^2 / 2 m^* k_B T_e}). \quad (25)$$

The quantity that appears in the expression for the rate is the square modulus

$$\varepsilon(q, \omega)^2 = (\varepsilon_{LR} + \varepsilon_{eR})^2 + (\varepsilon_{LI} + \varepsilon_{eI})^2. \quad (26)$$

Approximate analytic results for the strictly 2D case have been obtained previously with the assumption that the integral in Eq. (21) can be evaluated for  $u \approx 1$ , which maximises the exponential factor.<sup>27,29</sup> Here we make no such approximations. The integral is evaluated numerically.

The net energy exchange rate is determined mainly by substantial energy exchanges, even though these are not the most rapid. This may be seen by expressing Eq. (21) as follows:

$$W(k, k') = W_0 J_{\pm}(\varpi) e^{\varpi/2}, \quad (27)$$

where  $J_{\pm}(\varpi)$  is the integral, which is dependent of the sign of the energy exchange through the denominator of  $\gamma$  [Eq. (21)]. Noting that  $\varpi > 0$  implies loss of energy and  $\varpi < 0$  gain, we see that the net loss of energy by the incident electron is

$$Q = Q_0 \left( \int_0^{E/k_B T} \varpi e^{\varpi/2} J_+(\varpi) d\varpi - \int_0^{\infty} \varpi e^{-\varpi/2} J_-(\varpi) d\varpi \right),$$

$$Q_0 = \frac{e^4 n}{16 \pi^{3/2} \hbar \varepsilon_{\infty}^2}. \quad (28)$$

Small energy exchanges contribute little to the integral [the factor  $\varpi^{3/2}$  in the denominator of  $J(\varpi)$  notwithstanding]. When  $\varpi \ll 1, J_+ \approx J_-$  and when  $\varpi \gg 1$  the second integral in Eq. (28) is small and there will be little error in replacing the upper limit by  $E/k_B T$ . Thus, Eq. (28) can be simplified for superthermal electrons as follows:

$$Q = Q_0 \int_0^{E/k_B T} 2 \varpi \sinh(\varpi/2) J_+(\varpi) d\varpi. \quad (29)$$

## VI. RESULTS

The equations derived in the previous sections will now be applied to a particular case, one that is relevant to the problem of hot-electron transport in GaN heterostructures at low lattice temperatures where it has been suggested<sup>22</sup> that, in the absence of charged-impurity scattering, electron-electron scattering may be strong enough to allow the unprecedented situation of a drifted Maxwellian distribution to occur leading to the phenomenon of ‘‘squeezed electrons.’’ We consider a GaN heterostructure at a lattice temperature of 77 K containing a hot, nondegenerate electron gas with

TABLE I. GaN properties.  $c_L = \frac{1}{3}(2c_{11} + c_{33}) - \frac{2}{15}c_x$ ,  $c_T = c_{44} + \frac{2}{15}c_x$ ,  $c_x = c_{11} + c_{33} - 2c_{13} - 4c_{44}$ ,  $s_L = \sqrt{c_L/\rho}$ ,  $s_T = \sqrt{c_T/\rho}$ .

$\rho$ (g/cm <sup>3</sup> )	$\epsilon_s/\epsilon_0$	$\epsilon_\infty/\epsilon_0$	$m^*/m$	$\bar{\mu}$ (eV)			
6.15	9.0	5.35	0.23	8			
$c_{11}$ (GPa)	$c_{12}$ (GPa)	$c_{13}$ (GPa)	$c_{33}$ (GPa)	$e_{33}$ (C/m <sup>2</sup> )	$e_{31}$ (C/m <sup>2</sup> )	$e_{15}$ (C/m <sup>2</sup> )	
374	106	70	379	0.67	-0.37	-0.33	

Fang-Howard factor  $b = 4.8 \times 10^6/\text{cm}$ , density  $2.5 \times 10^{12} \text{ cm}^{-2}$ , and electron temperature 300 K. The choice of  $b$  and density (see the Appendix II), though consistent within a simple electrostatic model<sup>30</sup> for the specific structure  $\text{Al}_{0.3}\text{Ga}_{0.7}\text{N}(37 \text{ \AA})/\text{GaN}$ , is made chiefly to allow quantitative estimates of the orders of magnitude of the intrasubband rates involved, which is our main purpose here. At the electron temperature of 300 K the density of  $2.5 \times 10^{12} \text{ cm}^{-2}$  is the largest for nondegenerate statistics to apply.

In the momentum and energy relaxation rates for acoustic phonons the lattice temperature determines the number of excited phonons and the electron temperature affects the screening. The parameters used in the calculation are mainly those quoted in Ref. 2 and are shown in Table I. Figure 2 illustrates the nonpolar rates, and Fig. 3 the piezoelectric rates, as a function of the electron wave vector in units of the vector  $q_0 = \sqrt{2m^* \omega_{\text{LO}}/\hbar}$ , where  $\omega_{\text{LO}}$  is the optical-phonon

frequency, taken to be 92 meV. From elementary considerations we expect the ratio of the momentum-relaxation rate and the energy-relaxation rate ( $W_E/E$ ) to be close to  $2m^*s_\alpha^2/k_B T_L$ , i.e., 0.02 for LA modes and 0.008 for TA modes, which is the case near  $k/q_0 = 1$ . Figure 4 illustrates the extent of error introduced by using spherical averages of the piezoelectric coefficients.

Screening, to a large extent, has acted to equalize the nonpolar and piezoelectric rates at high  $k$ , but at low  $k$  the piezoelectric momentum relaxation rate is dominant. As regards energy relaxation, we note that absorption is dominant at low  $k$  for both interactions, leading to a slight negative rate in each case. The thermal wave vector, defined by  $k_T = \sqrt{2m^*k_B T/\hbar^2}$ , gives  $k/q_0 = 0.26$  at 77 K. Thus for  $k < k_T$  net absorption is favored and net emission is favored for  $k > k_T$ .

The combined acoustic phonon energy relaxation rate at  $k/q_0 = 1$  does not exceed  $2 \times 10^{-4} \text{ eV/ps}$ . This may be com-

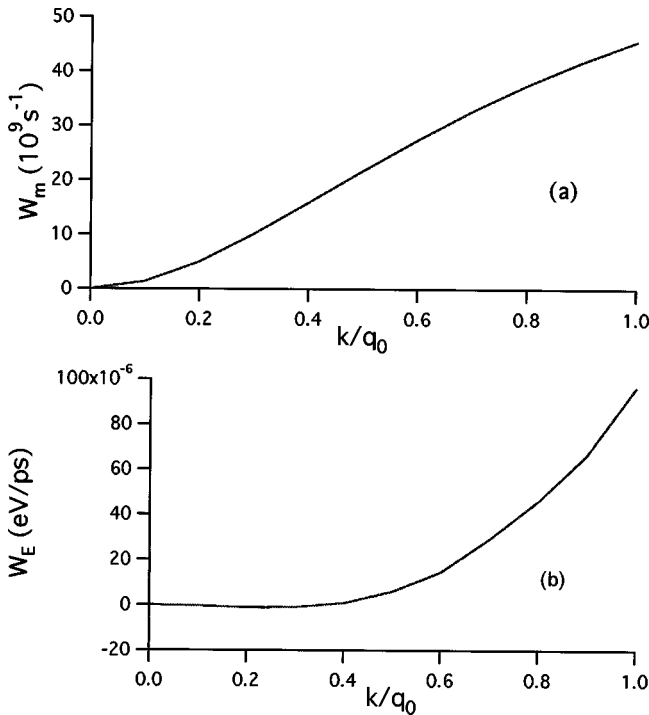


FIG. 2. Nonpolar acoustic-phonon rates in quasi-2D GaN: (a) momentum relaxation rate, (b) energy relaxation rate:  $k$  is the electron wave vector and  $q_0 = (2m^* \omega_{\text{LO}}/\hbar)^{1/2}$ . ( $T_L = 77 \text{ K}$ ,  $T_e = 300 \text{ K}$ ,  $n = 2.5 \times 10^{12} \text{ cm}^{-2}$ .)

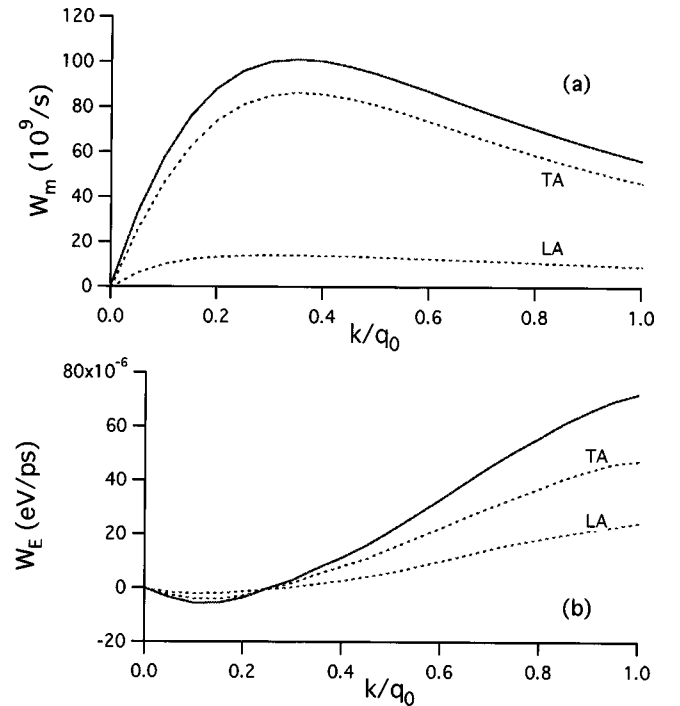


FIG. 3. Piezoelectric rates in quasi-2D GaN: TA, LA are transverse, longitudinal modes. (a) Momentum relaxation rate, (b) energy relaxation rate:  $k$  is the electron wave vector and  $q_0 = (2m^* \omega_{\text{LO}}/\hbar)^{1/2}$ . ( $T_L = 77 \text{ K}$ ,  $T_e = 300 \text{ K}$ ,  $n = 2.5 \times 10^{12} \text{ cm}^{-2}$ .)

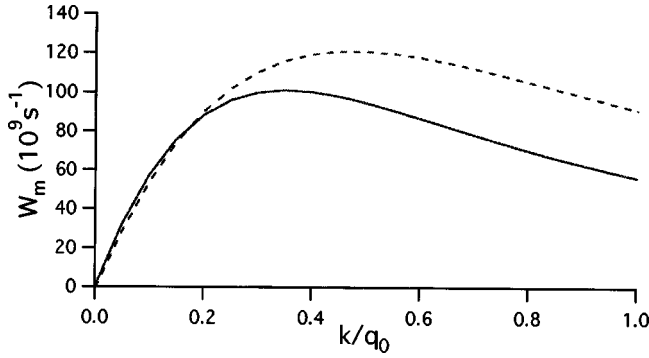


FIG. 4. Comparison of piezoelectric momentum relaxation rates (solid curve) with spherical-average approximation (dashed curve).

pared with the energy relaxation rate for optical phonons assuming a basic unscreened emission rate of  $10^{14}/s$ , a phonon energy of 92 meV, and a form factor  $f_0$  [Eq. (A1)] for  $q = q_0$ , giving 2.0 eV/ps, a factor  $10^4$  higher than the acoustic phonon rate.

Turning to the energy exchange associated with  $e-e$  scattering, we first consider the ideal 2D case. Figure 5 shows the energy rate as a function of amount of exchange energy according to Eq. (29) assuming the form factor to be unity. There is a broad resonance at low energies which is associated with the plasmon dispersion, and there are resonances at and above the phonon energy associated with coupled-mode dispersion. We have discussed the spectrum of energy exchange more fully elsewhere.<sup>32</sup> The total energy rate versus initial electron energy is shown in Fig. 6(a). Figures 7 and 8

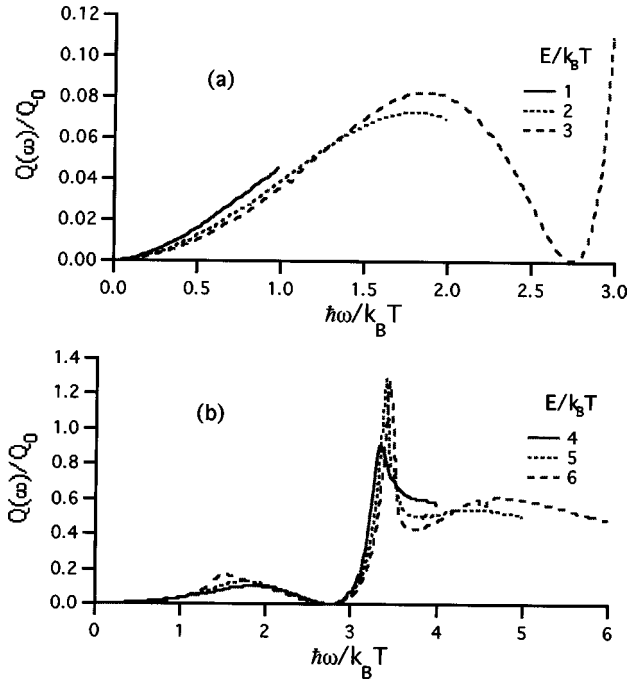


FIG. 5. Spectrum of electron-electron energy exchange rates for 2D GaN [integrand of Eq. (29)]. The energy exchanged is  $\hbar\omega$ ,  $E$ =incident electron energy,  $T=300$  K,  $n=2.5 \times 10^{12} \text{ cm}^{-2}$ ,  $Q_0 = 4.88 \text{ eV/ps}$ : (a) low energies, (b) full range.

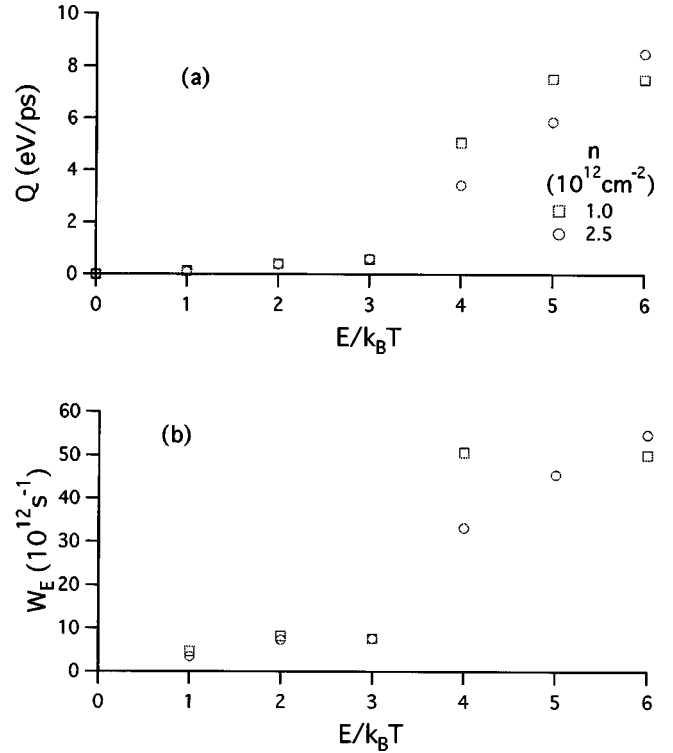


FIG. 6. Total electron-electron rates,  $Q$  [Eq. (29)], for 2D GaN at 300 K with  $n=1.0$  or  $2.5 \times 10^{12} \text{ cm}^{-2}$ . (a) Energy relaxation. (b) Momentum-relaxation rate ( $Q/E$ ).

show the result of incorporating the form factor. Including the form factor reduces the rates at low energies by a factor of 2, approximately. This reduction is less than might have been expected basically because the form factor appears both in the bare interaction and in the dielectric function; it therefore reduces the bare interaction (by a factor of about 4) but it also reduces the screening. Using the correct equation for energy relaxation, Eq. (28), reduces the rate at low energies but has little effect at high energies. Comparison with the energy relaxation rates associated with acoustic phonons may be facilitated by noting that  $E/k_B T=3$  corresponds to  $k/q_0=0.92$ . Around this energy the electron rate is about  $3 \times 10^{-1} \text{ eV/ps}$  which is to be compared with  $2 \times 10^{-4} \text{ eV/ps}$  for the acoustic phonon rate, which confirms that the electron-electron rate is much bigger leading to the establishment of an electron temperature (implicitly assumed in our choice of distribution function). The rate for electron-electron scattering at energies above the optical-phonon energy increases to around 2 eV/ps, which is comparable with that for optical phonon scattering (2 eV/ps), making our assumption of an electron temperature at higher energies more questionable.

A rough measure of momentum relaxation rate which is adequate for purposes of comparison with the phonon rates is the energy relaxation rate  $W_E = Q/E$ , with  $Q$  defined by Eq. (29) and  $E$  is the initial energy, shown in Fig. 6(b). Below the optical-phonon energy this rate (reduced by the form factor) is around  $3 \times 10^{12}/s$ , which is to be compared with  $10^{11}/s$ , the momentum relaxation rates associated with acoustic

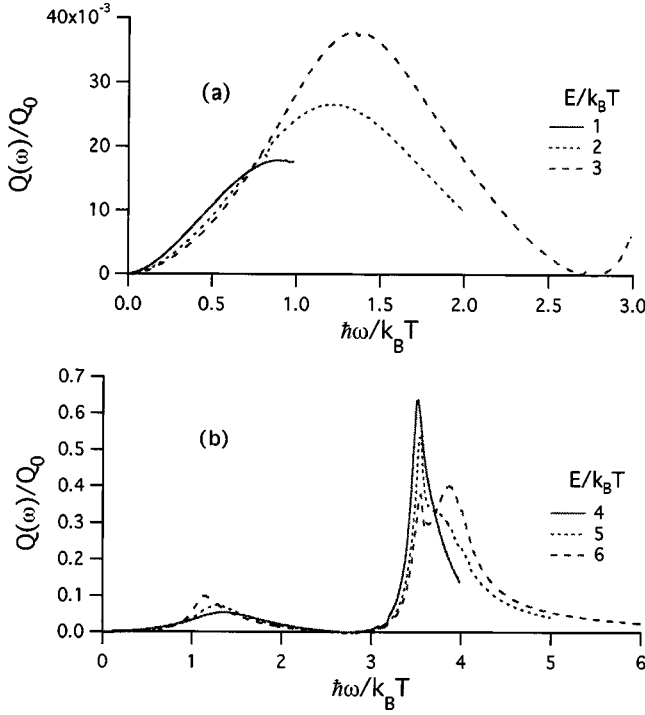


FIG. 7. Spectrum of electron-electron energy exchange rates for quasi-2D GaN (including form factor). Notation and conditions as in Fig. 5.

phonons. In general, for mobilities significantly in excess of around  $2500 \text{ cm}^2/\text{V s}$  the hot-electron distribution would be a drifted Maxwellian. Above the phonon energy the rate ( $\approx 2 \times 10^{13}/\text{s}$ ) is comparable with the optical-phonon rate ( $\approx 10^{14}/\text{s}$  divided by 4).

## VII. CONCLUSION

In the particular case studied (lattice temperature 77 K, electron temperature 300 K, electron density of order  $10^{12} \text{ cm}^{-2}$ , GaN heterostructure) we can conclude that an electron temperature is easily established for energies less than the optical-phonon energy, and conditions in which a drifted Maxwellian distribution is established are far from being impracticable. We further note that our results are insensitive to electron density above  $1 \times 10^{12} \text{ cm}^{-2}$ , an insensitivity that is expected to extend into the degenerate regime. In practical structures, where densities are typically in the range  $10^{12} - 10^{13} \text{ cm}^{-2}$  but mobilities are typically less than  $2000 \text{ cm}^2/\text{V s}$  even at low temperatures, a drifted Maxwellian is not predicted, but the establishment of an electron temperature, at least at low energies, is predicted. In some cases low-temperature mobilities over  $10000 \text{ cm}^2/\text{V s}$  have been observed<sup>33</sup> so drifted Maxwellians are to be expected along with the related transport phenomena described in Ref. 22. However, it is then necessary to return to the calculation of the dynamics of  $e-e$  collisions and to incorporate a drifted Maxwellian in place of the isotropic distribution used in our analysis.

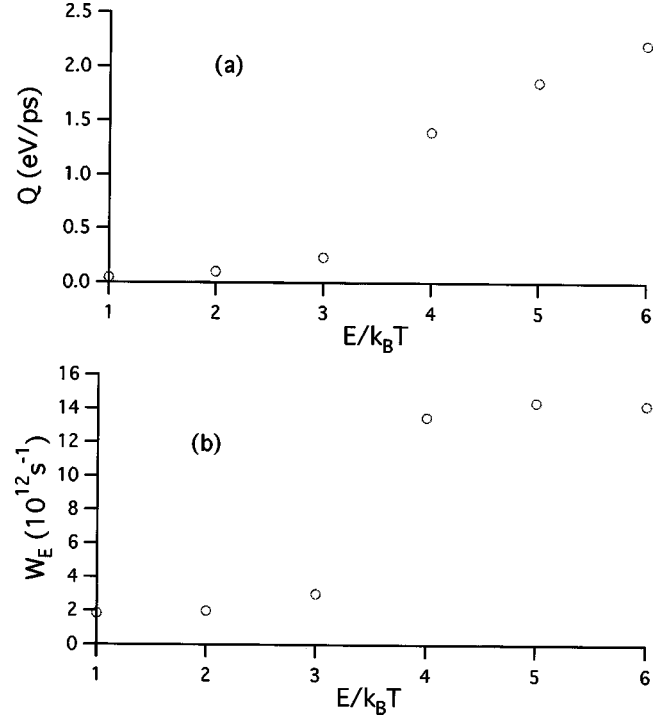


FIG. 8. Total electron-electron rates for quasi-2D GaN (including form-factor) at 300 K for  $n = 2.5 \times 10^{12} \text{ cm}^{-2}$ .

## ACKNOWLEDGMENTS

We are grateful for the support of the US Office of Naval Research through Award No. N00014-01-1-0002 sponsored by Dr. Colin Wood.

## APPENDIX

### 1. Piezoelectric form factors

The form factors arising from the anisotropy of the piezoelectric interaction with electrons described by the Fang-Howard wave function are given by

$$f_n = \int_0^\infty dz \int_0^\infty dz' \psi^2(z) \psi^2(z') (q|z-z'|)^n e^{-q|z-z'|},$$

$$f_0 = \frac{8+9r+3r^2}{8(1+r)^3}, \quad f_1 = \frac{3r(5+4r+r^2)}{8(1+r)^4},$$

$$f_2 = \frac{3r^2(8+5r+r^2)}{4(1+r)^5}, \quad f_3 = \frac{3r^3(35+18r+3r^2)}{4(1+r)^6}. \quad (\text{A1})$$

where  $r = q/b$ .

### 2. Model heterostructure

A simple electrostatic model that captures the essence of how the spontaneous and piezoelectric polarization in a heterostructure induces a quasi-2D electron gas results in the following equation for the electron charge density.<sup>30</sup>

$$\sigma = (1 + \eta)^{-1} [\sigma_{p1} - \sigma_{p2} - \phi(\epsilon_2/a_2 + \epsilon_1/a_1)],$$

$$\eta = \epsilon_1 \pi \hbar^2 / e^2 m^* a_1. \quad (\text{A2})$$

Here, subscripts 1 and 2 refer to the barrier and GaN, respectively,  $\epsilon_{1,2}$  is the permittivity,  $a_{1,2}$  is the thickness, and  $\phi$  is the GaN Schottky barrier ( $\approx 0.8$  eV). For a  $\text{Al}_{0.3}\text{Ga}_{0.7}\text{N}$  barrier we have taken the polarization charge density, spontaneous plus piezoelectric, to be  $0.055 \text{ C/m}^2$  and the spontaneous

charge density in the GaN to be  $0.029 \text{ C/m}^2$ .<sup>1</sup> (Note that later estimates give a magnitude 9% larger<sup>31</sup> a difference that is unimportant in the present context.) For an electron density at an electron temperature of 300 K that is still mainly non-degenerate (i.e.,  $n = 2.5 \times 10^{12} \text{ cm}^{-2}$ ) the barrier width should be about  $37 \text{ \AA}$  with  $a_2$  large. The resulting field in the triangular well then defines the lowest subband energy from which the Fang-Howard parameter  $b$  can be deduced. Obviously, there is plenty of room here for more sophisticated modeling.

- 
- <sup>1</sup>F. Bernardini, V. Fiorentini, and D. Vanderbilt, Phys. Rev. B **56**, R10 024 (1997).  
<sup>2</sup>O. Ambacher, J. Smart, J. R. Shealy, N. G. Weimann, K. Chu, M. Murphy, W. J. Schaff, and L. F. Eastman, J. Appl. Phys. **85**, 3222 (1999).  
<sup>3</sup>O. Ambacher, B. Foutz, J. Smart, J. R. Shealy, N. G. Weimann, K. Chu, M. Murphy, A. J. Sierakowski, W. J. Schaff, L. F. Eastman, R. Dimitrov, A. Mitchell, and M. Stutzmann, J. Appl. Phys. **87**, 334 (2000).  
<sup>4</sup>D. Jena, A. C. Gossard, and U. K. Mishra, J. Appl. Phys. **88**, 4734 (2000).  
<sup>5</sup>V. W. L. Chin, B. Zhou, T. L. Tansley, and X. Li, J. Appl. Phys. **77**, 6064 (1995).  
<sup>6</sup>B. K. Ridley, Phys. Status Solidi A **176**, 359 (1999).  
<sup>7</sup>R. Loudon, Adv. Phys. **13**, 423 (1964).  
<sup>8</sup>B. C. Lee, K. W. Kim, M. Dutta, and M. A. Strocio, Phys. Rev. B **56**, 997 (1997).  
<sup>9</sup>C. Bulutay, B. K. Ridley, and N. A. Zakhleniuk, Phys. Rev. B **62**, 15 754 (2000).  
<sup>10</sup>B. K. Ridley, N. A. Zakhleniuk, and M. Babiker, Solid State Commun. **116**, 385 (2000).  
<sup>11</sup>B. K. Ridley, J. Phys.: Condens. Matter **14**, 3469 (2002).  
<sup>12</sup>B. K. Ridley, Proc. SPIE **1675**, 492 (1992); Phys. Rev. B **47**, 4592 (1993).  
<sup>13</sup>N. Mori and T. Ando, Phys. Rev. B **40**, 6175 (1985).  
<sup>14</sup>D. R. Anderson, M. Babiker, C. R. Bennett, N. A. Zakhleniuk, and B. K. Ridley, J. Phys.: Condens. Matter **13**, 5999 (2001).  
<sup>15</sup>T. Kawamura and S. Das Sarma, Phys. Rev. B **45**, 3612 (1992).  
<sup>16</sup>S.-C. Lee and I. Galbraith, Phys. Rev. B **59**, 15 796 (1999).  
<sup>17</sup>M. G. Kane, Phys. Rev. B **54**, 16 345 (1996).  
<sup>18</sup>M. Shur, B. Gelmont, and M. A. Khan, J. Electron. Mater. **25**, 777 (1996).  
<sup>19</sup>L. Hsu and W. Walukiewicz, Phys. Rev. B **56**, 1520 (1997).  
<sup>20</sup>N. A. Zakhleniuk, C. R. Bennett, B. K. Ridley, and M. Babiker, Appl. Phys. Lett. **73**, 2485 (1998).  
<sup>21</sup>B. K. Ridley, B. E. Foutz, and L. F. Eastman, Phys. Rev. B **61**, 16 862 (2000).  
<sup>22</sup>B. K. Ridley and N. A. Zakhleniuk, Int. J. High Speed Electron. Syst. **11**, 479 (2001); *Topics in High Field Transport in Semiconductors*, edited by K. F. Brennan and P. P. Ruden (World Scientific, Singapore, 2001), p. 117.  
<sup>23</sup>P. J. Price, Ann. Phys. (N.Y.) **133**, 217 (1981).  
<sup>24</sup>F. F. Fang and W. E. Howard, Phys. Rev. **163**, 816 (1967).  
<sup>25</sup>J. D. Zook, Phys. Rev. A **136**, A869 (1964).  
<sup>26</sup>A. R. Hutson, J. Appl. Phys. **32**, 2287 (1961).  
<sup>27</sup>S. E. Esipov and I. B. Levinson, Sov. Phys. JETP **63**, 191 (1986).  
<sup>28</sup>J. R. Meyer and F. J. Bartoli, Phys. Rev. B **28**, 915 (1983).  
<sup>29</sup>B. K. Ridley, J. Phys.: Condens. Matter **13**, 2799 (2001).  
<sup>30</sup>B. K. Ridley, Appl. Phys. Lett. **77**, 990 (2000).  
<sup>31</sup>F. Bernardini, V. Fiorentini, and D. Vanderbilt, Phys. Rev. B **63**, 193201 (2001).  
<sup>32</sup>P. Tripathi and B. K. Ridley in *Proceedings of the International Conference on the Physics of Semiconductors 24, Edinburgh, July 2002* (to be published).  
<sup>33</sup>L. N. Pfeiffer, K. W. West, H. L. Stormer, and K. W. Baldwin, Appl. Phys. Lett. **55**, 1888 (1989).